International Journal of Power Electronics and Drive System (IJPEDS)
Vol. 11, No. 1, March 2020, pp. 367~373
ISSN: 2088-8694, DOI: 10.11591/ijpeds.v11.i1.pp367-373

Voltage tracking of bridgeless PFC Cuk converter using PI controller

W. M. Utomo[1], N. A. A. Isa[2], A. A. Bakar[3], A. F. H. A. Gani[4], B. E. Prasetyo[5], H. Elmunsyah[5], Y. M. Y Buswig[7]
[1,2,3,4] Department of Electrical Power Engineering (JEK), Faculty of Electrical and Electronics Engineering (FKEE), Universiti Tun Hussein Onn Malaysia, Malaysia
[5] Department of Electrical Engineering, Politeknik Negeri Malang, Indonesia.
[6] Department of Electrical Engineering, Universitas Negeri Malang, Indonesia.
[7] Department Electrical and Electronic Engineering, Faculty of Engineering, Universiti Malaysia Sarawak, Malaysia

Article Info

Article history:

Received Sep 8, 2019
Revised Nov 14, 2019
Accepted Dec 7, 2019

Keywords:

Bridgeless
Power factor correction
Cuk converter
Control system
Proportional-Integral

ABSTRACT

This paper proposes a Proportional-Integral (PI) control voltage tracking of Bridgeless Power Factor Correction (BPFC) Cuk converter. In order to investigate the behaviour of different output voltages during overshoot, steady state and step response, P.I controller is designed to set the -42 V, -48 V, -54 V output voltages. The simulation results show that the proposed PI controller able to control the output voltage and achieve fast steady state and step response of BPFC Cuk converter. When the value of output voltage increase, the overshoot voltage will become higher but the steady state respond will be faster. Furthermore, BPFC Cuk converter with P.I controller have low output voltage ripples.

Corresponding Author:

Wahyu Mulyo Utomo,
Departement of Electrical and Electronic Engineering,
Universiti Tun Hussein Onn Malaysia,
86400, Parit Raja, Johor, Malaysia.
Email: wahyu@uthm.edu.my

1. INTRODUCTION

Power electronic equipment with an active power factor correction (PFC) for telecom, datacom, and automotive electrical system are becoming necessary nowadays [1-5]. There are several types of DC-DC BPFC converters were developed for PFC applications such as boost, buck, buck-boost, SEPIC and Cuk converters [6]. However, for low power application, BPFC Cuk converter is the most reliable converter because it offers low THD of input current, good power factor, easy to implement in transformer isolation, and natural protection against inrush current from start-up or overload current [7-11]. This converter acts similar to the buck-boost converter since it able to step up and step-down the output voltage by controlling the duty cycle [11, 12]

Basically, the DC-DC converter used power semiconductor devices that operated as the electronic switches which are refer as switched mode power supply [SMPS] [13, 14]. The operation of this switching devices may cause inherently nonlinear characteristic of the BPFC Cuk converter [15]. Pulse width modulation (PWM) is the most popular method for the various switching technique [15, 16]. Switch-mode PWM dc–dc converters used to provide a constant output voltage[17]. Proportional-Integral (PI)

controller often to use as the control method for PWM switching due to the simple design and easy to implement [18, 19].

The proposed system bridgeless PFC Cuk converter is shown in Figure 1 where, a single MOSFET switch replacing the two MOSFETs, which helps to reduce high conduction loss and size of the structure [20, 21]. In this case, the structure proposed to reduce the complexity of controller circuit. Basically, bridgeless PFC structure suffer from the difficulty of implementation of control circuit because of two switches. Nevertheless, this structure can reduce conduction losses form bridgeless. In this paper, the output voltage was selected to -42 and -54 V for the electric vehicle application [22-24]. Meanwhile -48 V is used in telecommunication application[7, 25].

The remainder of this study is organized as follows: operation of BPFC Cuk converter will be shown in section II. Then the parameter design for PFC converter is presented in section III. Section IV describe about the P.I controller for BPFC Cuk converter. Simulation result and analysis in section V, followed by conclusion in section VI.

2. OPERATION OF BPFC CUK CONVERTER

The proposed BPFC Cuk structure as shown in Figure 1. When the MOSFET *M* is turned-on during positive cycle, D_p, D_1 are on-state and D_{out} is off-state as shown in

Figure 2. There are two modes for this operation. For the first mode, the inductors L_1 and L_2 are charging. Meanwhile, the capacitor C_1 and capacitor C_2 are discharging. Then output inductor L_o is charging and capacitor C_{out} is discharging. In mode 2 condition, capacitor C_1 and capacitor C_2 are charging through inductors L_1 and L_1. Then, the inductor L_{out} recharges the capacitor C_{out}.

When the MOSFET M is turned-on during negative cycle, D_n, D_2 operate in on-state and D_{out} is off-state as shown in Figure 3. There are two modes for this operation. First, the inductors L_1 and L_2 are charging, the capacitor C_1 and capacitor C_2 are discharging, the output inductor L_o is charging and capacitor C_{out} is discharging. For the next condition, capacitor C_1 and capacitor C_2 are charging through inductors L_1 and L_1. Then, the inductor L_{out} recharges the capacitor $C_{out\ and}$ power supplied to the load.

When the MOSFET M is turned-off, D_p, D_1 are off-state and D_{out} is on-state as shown in

Figure 4. There are four conditions for this mode. In the first condition, capacitor C_1 and capacitor C_2 are charging. Inductors L_1 and L_2 are discharging. Then, the output inductor L_{out} is discharging while, capacitor C_o is charging and the power is supplied to the load. For the second condition, inductor L_1, inductor L_2 and capacitor C_2 are discharging. Then, inductor L_1, inductor L_2 and capacitor C_2 are discharging, while capacitor C_1 is charging. Output inductor L_{out} is discharging and capacitor C_{out} is charging and the power is supplied to the load. For the third condition, inductor L_1, inductor L_2 and capacitor C_2 are discharging. Meanwhile capacitor C_1 is charging. Then, capacitor C_{out} is discharging through output inductor L_{out} and the power is supplied to the load. For the fourth condition, capacitor C_1 and capacitor C_2 are discharging through inductors L_1. Then, L_2 are charging and output inductor L_{out} recharges capacitor C_{out}. Then, the power is supplied to the load.

When the MOSFET M is turned-off, D_n, D_2 are in off-state while D_{out} is on-state as shown in Figure 5. There are four modes at this condition. First, capacitor C_1 and capacitor C_2 are charging, at the same time inductors L_1 and L_2 are discharging. Then, the output inductor L_{out} is discharging, capacitor C_o is charging and the power is supplied to the load. In the second mode, inductor L_1, inductor L_2 and capacitor C_2 are discharging. Then, inductor L_1, inductor L_2 and capacitor C_2 are discharging while capacitor C_1 is charging. Output inductor L_{out} is discharging. Capacitor C_{out} is charging and power is supplied to the load. For the third mode, inductor L_1, inductor L_2 and capacitor C_2 are discharging, but capacitor C_1 is charging. Meanwhile, capacitor C_{out} is discharging through output inductor L_{out} and the power is supplied to the load. In the fourth mode, capacitor C_1 and capacitor C_2 are discharging through inductors L_1. Then, L_2 is in charging mode. However, inductor L_{out} recharges the capacitor C_{out} and the power is supplied to the load.

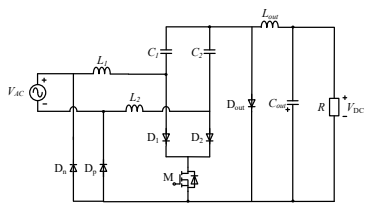

Figure 1. BPFC cuk structure

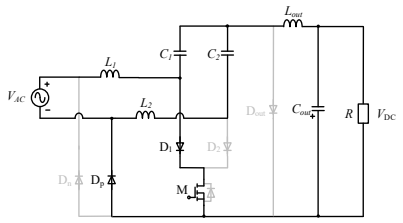

Figure 2. MOSFET turned-on during positive cycle

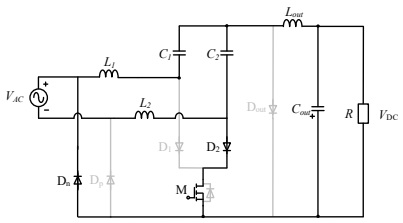

Figure 3. MOSFET turned-on during negative cycle

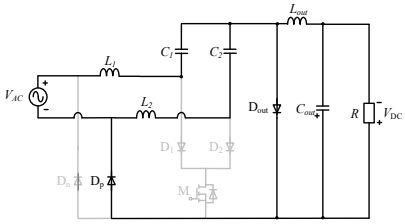

Figure 4. MOSFET turned-off during positive cycle

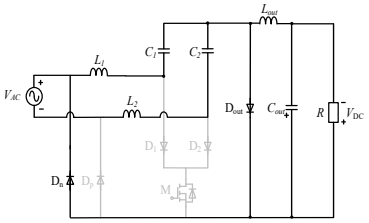

Figure 5. MOSFET turned-off during negative cycle

3. PARAMETER DESIGN FOR BPFC CUK CONVERTER

3.1. Voltage conversion ratio, M

The voltage conversion ratio M = V_o/V_m in terms of circuit structure parameters can be obtained by applying the power-balancing principle where $P_{in} = P_{AC}$ by assuming a lossless converter.

$$P_{AC} = \frac{2}{T}\int_0^{\frac{T}{2}} V_{AC}(t) \cdot I_{AC}(t)\, dt \tag{1}$$

The average AC supply current is given as (2),

$$I_{AC}(t) = \frac{V_{AC}(t)}{R_e} \tag{2}$$

Where the R_e is defined as the effective input resistance of the converter and given by (3)

$$R_e = \frac{2 \cdot L_e}{D_{ton}{}^2 \cdot T_S} \tag{3}$$

The D_{ton} is the summation of D_{1Ts} and D_2T_s. On the other hand, the average output current of diode during one-line cycle is equal to the average current, I_o through to the load, R

$$I_o = \frac{V_{out}}{R} \tag{4}$$

Thus, it can be simplified by evaluating (2) by using (3) and applying the power-balancing between the AC supply and DC output, the voltage conversion ratio is equal to:

$$M = \frac{V_{out}}{\sqrt{2} \cdot V_{AC}} = \sqrt{\frac{R}{2 \cdot R_e}} = \frac{D_{ton}}{\sqrt{2 \cdot K_e}} \tag{5}$$

3.2. Gain ratio as function of duty cycle, D

DCM operation mode requires that the sum of duty cycle and the normalized MOSFET-off time length to be less than one. Following inequality must be satisfied:

$$D_{toff} < 1 - D_{ton} \tag{6}$$

Where the D_{toff} is the summation of D_3T_s and D_4T_s. The worst situation occurs at ωt = 90º. Therefore, to operate in DCM operation

$$D = \frac{M}{M+1} \tag{7}$$

3.3. Design of input inductor L_1 and L_2

The input inductance is calculated by using inductor current ripple:

$$\Delta I_{L1} = \frac{\sqrt{2}\cdot V_{AC}}{2\cdot L_1} \cdot D \cdot T_s \tag{8}$$

The maximum inductor current ripple calculated from the peak input current is given by (9)

$$\Delta IAC, peak = \left(\frac{2\cdot P_{AC}}{\sqrt{2}\cdot V_{AC}}\right)_{L1,max} \tag{9}$$

By substituting (9) into (10), the input inductance L_1 can be calculated. Noted that, the L_1 is equal to L_2, thus the same formula can be used. The value of input inductance can be found as:

$$L_1 = \frac{V_{AC}\cdot D}{\Delta I_{L1}\cdot f_{sw}} \tag{10}$$

3.4. Design of output inductor, L_o

From (1), the average output current of diode, I_{Do} during one line-cycle of the AC supply can be determined by (11)

$$I_{AC,Avg} = \frac{D_{ton}\cdot T_s\cdot V_{AC}^2}{2\cdot L_e\cdot V_o} \tag{11}$$

K_e is dimensionless parameter are defined and can be expressed by (12)

$$K_e = \frac{D^2}{2\cdot M^2} \tag{12}$$

The average output current is the average diode current, L_e from can be found by (13)

$$L_e = \frac{R\cdot T_S\cdot K_e}{2} \tag{13}$$

Therefore, the output inductor can be determined by applying (10) and (13):

$$L_o = \frac{L_1\cdot L_e}{L_1 - L_e} \tag{14}$$

3.5. Design of input capacitor, C_1 and C_2

The input capacitor, C_1 is an important component in the Cuk topology since it may distort the quality of AC supply current. The C_1 must be designed properly by considering resonant frequency, f_r not close to line frequency f_L and switching frequency f_{sw}. Hence, the energy transfer to capacitor C_1 is determined based on inductors L_1, L_2, and L_o values. In addition, a better initial estimation for choosing the resonant frequency, f_r is given by (15). Noted that, the C_1 is equal to C_2 which the same formula can be used, thus the design C_1 (16) is:

$$f_L < f_r < f_{sw} \tag{15}$$

$$C_1 = C_2 = \frac{1}{(2\pi\cdot f_r)^2\cdot(L_1 + L_o)} \tag{16}$$

3.6. Design of output capacitor, C_o

Since the input of converter is AC supply, the output capacitor must be large enough to reduce the output voltage ripple. Thus, the output ripple frequency of the converter is two times of the input frequency, given in (15). In the worst case, the output current during half-period of the ripple frequency is provided by

the output capacitor. Therefore, the output voltage ripple must be selected based on the application requirement and C_o can be obtained as follows:

$$2\Delta f_{out} = f_L \tag{17}$$

$$C_o = \frac{P_{out}}{4 \cdot f_L \cdot V_o \cdot \Delta V_o} \tag{18}$$

4. PI CONTROLLER FOR BPFC CUK CONVERTER

Figure 6 illustrate the simulation diagram of proposed design of P.I controller for BPFC Cuk converter by using Maltab software. The reference voltage for P.I controller is set to -48V with 2/50 gain value. The value of P is 1.0 while the value of I is 3.34. The output of the P.I control is a power value and in order to convert it to a quantity that is comparable to that of the control signal, it goes through a power to PWM signal converter.

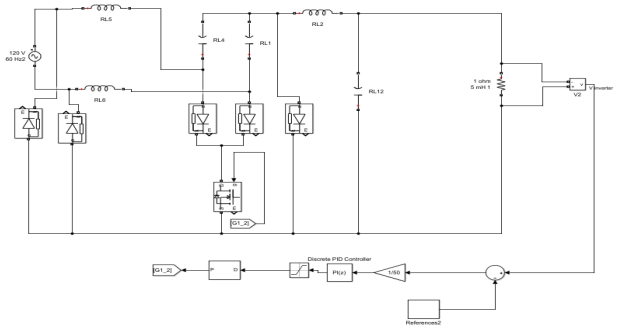

Figure 6. Simulation diagram of proposed BPFC Cuk with PI controller

5. SIMULATION RESULT

The performance of BPFC Cuk converter is verified by the simulation results by using MATLAB software. The converter is designed by the following specifications:

- Input voltage, V_{AC} = 230 V
- Output voltage, V_{DC} = -42 V, -48 V, -54 V
- Output power, P_{out} = 200 W
- Switching frequency, f_{sw} = 50 Hz
- Maximum output voltage ripple, ΔV_{out} = < 2V

Figure 7 show the characteristic of BPFC Cuk converter output voltage with P.I controller when the reference voltage is set up to -42V output voltage. The result shows the P.I controller functional well since the BPFC Cuk converter produce -42 V output voltage by following the reference voltage command. The overshoot voltage is -56 V. At 0.6 seconds, the system achieved steady state condition.

When the reference voltage for P.I controller is set to -48 V, the BPFC Cuk converter will produce -48 V output voltage as shown in Figure 8. The overshoot voltage is -59 V. The steady state condition achieved at 0.5 seconds.

Figure 9 illustrate the -54 V output voltage with P.I controller. The overshoot voltage is -63 V. For -54 V output voltage, the system starts to achieve stability at 0.41 seconds (Figure 10).

Figure 1 show the result for the output voltage ripple value with P.I controller. As increase the output voltage, the ripple will be increase too. P.I control is functioning well in order to reduce the output voltage ripples.

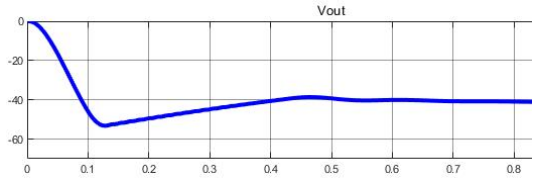

Figure 7. The output voltage versus time waveform when the reference voltage is -42V

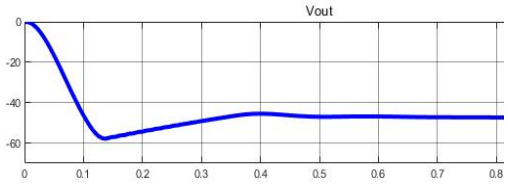

Figure 8. The output voltage versus time waveform when the reference voltage is -48V

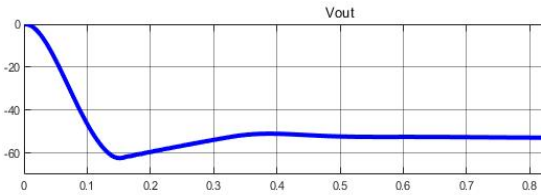

Figure 9. The output voltage versus time waveform when the reference voltage is -54V

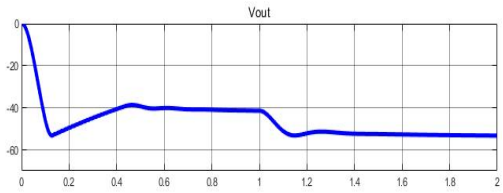

Figure 60. The output voltage versus time waveform when the reference voltage step-down from -42 V to -54 V

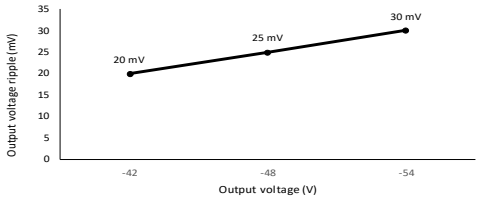

Figure 11. Output voltage ripple versus output voltage

6. CONCLUSION

In this paper, a proportional-integral control for bridgeless PFC Cuk converter is discussed. Various output voltage was set up to observe the characteristic of output voltage during steady state and step response. The proposed design of P.I controller able to control the output voltage of BPFC Cuk converter. As increase the output voltage value, the overshoot voltage will increase too but the steady state time will be faster. Furthermore, the performance of BPFC Cuk converter become better since the output voltage able to achieve fast steady state condition. The output voltage ripples are affected toward the output voltage value. However, the P.I controller able to reduce the output voltage ripples.

ACKNOWLEDGEMENTS

The authors would like to express their deepest appreciation to the Ministry of Higher Education (MOHE) Malaysia and Universiti Tun Hussein Onn Malaysia for supporting this research under research fund UTHM by using Geran Penyelidikan Pascasiswazah (GPPS) Vot. H309 and Power Electronic Converters Focus Group (PEC), Department of Electrical Power Engineering, Faculty of Electrical and Electronic Engineering, UTHM to undertake this research activity.

REFERENCES

[1] A. A. Fardoun, E. H. Ismail, M. A. Al-Saffar, and A. J. Sabzali, "New 'real' bridgeless high efficiency AC-DC converter," in *Conference Proceedings - IEEE Applied Power Electronics Conference and Exposition - APEC*, pp. 317-323, 2012.

[2] H. Nene, C. Jiang, and S. Choudhury, "Control for light load efficiency and THD improvements in PFC converter," pp. 1785-1788, 2017.
[3] B. Mangu and B. G. Fernandes, "Efficiency improvement of solar-wind based dual-input Cuk-SEPIC converter for telecom power supply," *IECON Proc. (Industrial Electron. Conf.*, pp. 978-983, 2012.
[4] K. C. Lee and B. H. Cho, "Low cost power factor correction (PFC) converter using delay control," *Power Convers. Conf. - Nagaoka 1997, Proc.*, vol. 1(Sep), pp. 335-340, 1997.
[5] A. Cocor, A. F. Member, A. Popescu, D. Stoichescu, and S. Oprea, "*Power supply blocks with cúk and self - lift cúk converters for telecommunication sites*," 2014.
[6] H. Z. Azazi, S. M. Ahmed, and A. E. Lashine, "High power factor and regulated output voltage for three-phase AC-DC converter using single-switch CUK converter," *2017 19th Int. Middle-East Power Syst. Conf. MEPCON 2017 - Proc.*, pp. 43-51, 2018.
[7] H. T. Yang, H. W. Chiang, and C. Y. Chen, "Implementation of bridgeless cuk power factor corrector with positive output voltage," *IEEE Trans. Ind. Appl.*, vol. 51, No. 4, pp. 3325-3333, 2015.
[8] D. S. L. Simonetti, J. Sebastian, and J. Uceda, "The discontinuous conduction mode sepic and cuk power factor preregulators: analysis and design," *IEEE Trans. Ind. Electron.*, vol. 44, No. 5, pp. 630-637, 1997.
[9] M. Brkovic and S. Cuk, "Input current shaper using cuk converter," *[Proceedings] Fourteenth Int. Telecommun. Energy Conf. - INTELEC '92*, pp. 532-539, 1992.
[10] S. Rakshit and J. Maity, "Fuzzy logic controlled ćuk converter," *2018 Int. Conf. Commun. Signal Process,* pp. 771-775, 2018.
[11] A. H. Abedin and A. Choudhury, "*Input switched single phase high performance bridgeless CÛK AC-DC converter*," 2012.
[12] M. K. R. Noor *et al.*, "Optimization of PFC SEPIC converter parameters design for minimization of THD and voltage ripple," *Int. J. Eng. Technol.*, vol. 7, No. 1, pp. 240-245, 2018.
[13] W. M. Utomo, S. S. Yi, Y. M. Y. Buswig, Z. A. Haron, A. A. Bakar, and M. Z. Ahmad, "Voltage tracking of a DC-DC flyback converter using neural network control," *International Journal of Power Electronics and Drive System (IJPEDS)*, vol. 2, No. 1, pp. 35-42, 2012.
[14] W. A. Y. Salah and S. Taib, "Improvement of transformerless 200W SMPS using CUK DC-DC converter," pp. 497-500, 2006.
[15] I. Engineering, "Comparitive study of single phase power factor correction based on fixed and variable PWM techniques using bridgeless cuk converter," pp. 290-295, 2018.
[16] B. Abdelhamid, L. Radhouane, and A. Bilel, "*Real time implementation of perturb and observe algorithm and PI controller for DC/DC converter*," 2017.
[17] Y. Liu, Y. Sun, and M. Su, "A control method for bridgeless cuk/sepic PFC rectifier to achieve power decoupling," *IEEE Trans. Ind. Electron.*, Vol. 64, No. 9, pp. 7272-7276, 2017.
[18] Y. Jang and M. M. Jovanović, "A new, soft-switched, high-power-factor boost converter with IGBTs," *IEEE Trans. Power Electron.*, vol. 17, No. 4, pp. 469-476, 2002.
[19] Z. Chen, "PI and sliding mode control of a cuk converter," vol. 27, No. 8, pp. 3695-3703, 2012.
[20] A. J. Sabzali, E. H. Ismail, M. A. Al-Saffar, and A. A. Fardoun, "A new bridgeless PFC Sepic and Cuk rectifiers with low conduction and switching losses," *2009 Int. Conf. Power Electron. Drive Syst.*, pp. 550-556, 2009.
[21] H. Farzaneh-Fard and M. Mahdavi, "Bridgeless CUK power factor correction rectifier with reduced conduction losses," *IET Power Electron.*, vol. 5, No. 9, pp. 1733-1740, 2012.
[22] R. D. Belekar, S. Subramanian, P. V. Panvalkar, M. Desai, and R. Patole, "Alternator charging system for electric motorcycles," pp. 1759-1766, 2017.
[23] K. Williams, "*Hybrid vehicles, 42volt vehicle electrical systems and the implications for EMC technology*," 2004.
[24] D. Patil, "*A cuk converter based bridgeless topology for high power factor fast battery charger for electric vechicle application*," 2012.
[25] L. Ahmethodžić, "*Cascade SMC control of Ćuk converter for telecommunication systems power supply*," 2014.